

Maximum Boost PWM Control Technique of Three Phase ZSI Based Wind Energy Conversion Systems

Sanusi Alabi Kamilu¹, AbdulHakeem Mohammed¹, Bello Ummai¹, Solomon Ikuforiji¹, Adebayo Michael¹,
AbdulKadir Muyideen²

¹ Department of Electrical Engineering, Waziri Umaru Federal Polytechnic, Birnin Kebbi,
Kebbi State, Nigeria

² Department of Mechanical Engineering, Waziri Umaru Federal Polytechnic, Birnin Kebbi,
Kebbi State, Nigeria

Email: sanusielect@yahoo.com

ABSTRACT

The concept of interfacing power converters with Wind energy conversion systems (WECS) has tremendously assisted in improving the power-supply stability, quality and reliability. In the use of conventional traditional inverters, the need for dead time and the fact that both upper and lower switches of the same phase leg cannot be gated ON at the same time are major issues. The turning ON of both switches will lead to destruction of the device due to shoot-through condition. This paper explores a three phase Z-source inverter topology based on the distinct feature of the impedance network and eliminates the above-mentioned problems. It provides a magnificent single stage power conversion. The control of the ZSI is achieved using maximum PWM boost control scheme and simulated in MATLAB environment. This proposed topology is able to boost the inverter output voltage under low wind situation.

Keywords: Buck-Boost Factor, DC-link Voltage, Shoot-through, Traditional Inverters, Maximum Boost PWM Control, Wind Energy Conversion Systems.

I. INTRODUCTION

The world electricity demand is growing rapidly and as a result of increasing environmental concerns, many views renewable energy as a better solution to reduce greenhouse gas emission and preserve the earth for the future generations [1]. Demand for renewable energy sources is anticipated to rise significantly over the coming years. Wind, a free, clean and inexhaustible source of energy, is increasingly competitive with other energy sources. Wind energy conversion system (WECS) is becoming the most competitive form of electricity generation from renewable sources. Within the concept of WECS, the permanent magnet synchronous generator

(PMSG)-based WECS is more common due to its improved energy yield, enhanced reliability and lowered maintenance problems [2, 3]. The concept of interfacing power converters with renewable energy systems has tremendously assisted in improving the power-supply stability, quality and reliability. The different configurations of power converters have been developed to interface the renewable resources for different applications. Power electronic converters have the capability of carrying out these tasks with greater efficiency. There exists two traditional inverters; voltage-source Inverter (VSI) and current-source Inverter (CSI) [4]. VSI has the following challenges; i. The inverter output voltage cannot be greater than the DC input voltage (buck converter) ii.

Additional voltage boost circuit is necessary, thereby increasing the cost of installation and also reducing the overall system reliability [5, 6]. CSI also has the following notional and theoretical problems; i. It is a boost inverter ii. It is costly iii. Poor power factor on the line side, iv. CSI is susceptible to Electromagnetic interference [4]. In both inverters, it is not allowed for the switches of the same leg to be turned ON at the same time, this is simply to avoid the occurrence of shoot through which will cause damage to the inverters [7, 8]. Due to the low characteristic nature of the wind energy at certain time, it is usually of common practice to interface a boost converter between the DC source and the traditional inverters as depicted in figure 1. This two-stage power conversion helps to maximise the output voltage of the inverter but it does come with problems like; increased system complexity, increased task to the controller, reduced system reliability due to more components counts and increased cost [5, 9]. Since the ON and OFF positions of the upper and lower switches of each phase leg are complementary in nature, it is necessary to include 'dead time' in each phase leg for protection purposes. If the dead time is not considered, it is possible for one switch to turn ON while the other is still in the process of turning OFF. The dead time in the reverse introduces harmonic problems and output voltage waveform distortions [6, 10-15].

However, in the recent past, researchers' attentions have been drifted towards developing new converter topologies for WEC applications. One of the most rising and competitive topology is the Impedance source inverter (ZSI) depicted in figure 2, which was firstly suggested in [16]. ZSI represents the driving force in achieving a high voltage, high power in today's renewable energy integration, most especially in wind energy conversion systems. Z-source inverters are employed as a better replacement to overcome the limitations of traditional VSI and CSI, such categories of inverters are controlled using pulse width modulation (PWM). The Z-source network

behaves as a second-order filter and provides an efficient means of limiting the voltage and current harmonics than the traditional inverters that uses large sizes of inductor (for CSI) and capacitor for (VSI) [16]. In contrast with other power electronics converters, its very uncommon feature is that, the output ac voltage can attain any value ranging from zero to infinity irrespective of the dc input voltage. It provides a magnificent single stage power conversion with buck-boost characteristics and shoot through immunity, with lowered cost, lowered volume and better efficiency [17, 18]. Thus, ZSI is a very appealing topology for WEC applications. It has also been proven in [14] that Z-source inverter can augment inverter conversion efficiency by 1% over the DC/DC boosted PWM traditional inverters.

The control schemes of the Z-source inverters are important issues towards achieving a high-quality power output. Several number of sinusoidal PWM control schemes have been proposed, they are utilised to control the output voltage of a ZSI by appropriate shoot through duty ratio. They are; simple boost control (SBC) [16, 19], maximum boost control (MBC) [17] and maximum constant boost control (MCBC) [20]. All of these control methods have their respective advantages and disadvantages [9].

Simple boost control (SBC) approach is very straightforward but the subsequent voltage stress across the switches is somewhat high as some traditional zero states are left unused [17, 19], this restricts attainable voltage gain due to the restriction on the device voltage rating [15]. Compared to Simple boost control, the potential area of operation of maximum boost PWM control scheme is more broader and moreover, a higher modulation index can be used, which means a lower voltage stress across the power switches [15]. However, this scheme injects a low frequency ripples in the inductor current and the capacitor voltage. This low output frequency will consequently lead to the need for higher value of inductors and capacitors. The maximum constant

boost control approach achieves the maximum voltage gain while still maintaining the shoot-through duty ratio constant. MCBC has the lowest phase current harmonics, lowest inductor current ripples and highest obtainable ac voltage but has a moderate control performance in the area of voltage stress and line voltage harmonics.

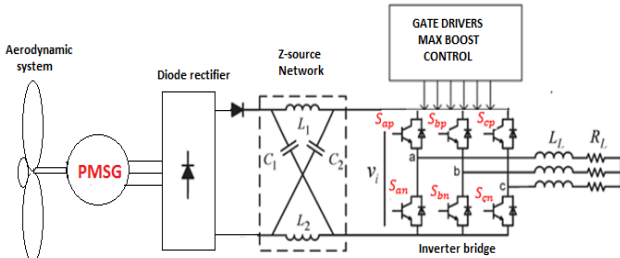


Figure 1. Traditional inverter with DC/DC Boost inverter for WECS

From the review analysis of the three control methods in [17], SBC has lowest performance characteristics. Though MBC has its own limitations compared to MCBC, but for the purpose of this research, MBC has been adopted because of its incredibly lowest stress on the power switches, lowest line voltage harmonics and a reasonably good efficiency.

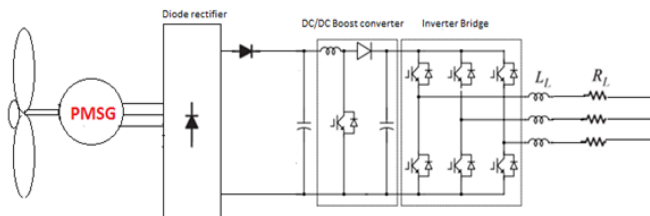


Figure 2. Z-source inverter for wind energy applications

In this paper, a three-phase Z-source inverter topology is presented as an interface with WECS. The control strategy of Z-source inverter is simulated in SIMULINK environment and implemented using Maximum Boost Controller which is used to sense, control, and optimize the performance of WECS. The maximum boost PWM signals are applied to the control operation of ZSI. This paper presents a detailed investigation of the proposed topology as shown in fig.2. Uncontrolled rectifier has been used for the ac/dc conversion because of its simplicity and

cost effectiveness. This paper is structured as follows. Section I presents an introduction on ZSI and its control schemes. Modelling of the aerodynamic and the drive train is presented in section II. Operation and analysis of ZSI is discussed in Section III. Section IV presents the proposed maximum boost PWM control strategy for the Z-source inverter. Simulation of results and discussions are presented in section IV and finally, the paper is concluded in Section VI.

II. MODELING OF WIND TURBINE WITH THE DRIVE TRAIN

Wind turbine is a device that uses the kinetic energy available in the wind to generate electricity. It is made up of rotating aero-dynamical blades positioned on a hub/shaft assembly, which convey the generated mechanical power from the rotor blade to electrical generator [21].

Mechanical output power (P_m) of the wind turbine is expressed in [22] as;

$$P_m = \frac{1}{2} \rho A v_w^3 C_p(\lambda, \beta) \tag{1}$$

The mechanical torque developed by the wind turbine T_m , and the tip speed ratio (λ) of the wind turbine are given by the following equations;

$$T_m = \frac{P_m}{\Omega} \tag{2}$$

$$\lambda = \frac{\Omega R}{v_w} \tag{3}$$

Where R is the turbine radius and Ω is the angular velocity (rad/sec) of the turbine. There are numbers of fitted equations for power coefficient, C_p , but a more generic one is given as [23];

$$C_p(\lambda, \beta) = \frac{0.5176 \left\{ \left(\frac{116}{\lambda_i} \right) - 0.4\beta - 5 \right\} e^{-\frac{21}{\lambda_i}} + 0.0068\lambda}{0.0068\lambda} \tag{4}$$

Where;

$$\lambda_i = \frac{1}{\lambda + 0.08\beta} - \frac{0.035}{1 + \beta^3}$$

In this research work, pitch angle β was set to zero.

Gear train is important in WECs due to the large speed difference between the wind turbine and the generator. In this paper, two mass model is considered. Figure 3 shows the schematic of two mass drive train. The turbine self-damping (D_t) is the aerodynamic resistance in the turbine blade. The generator self-damping (D_g) denotes mechanical friction and windage. The mutual damping (D_m) is the balancing dynamics that arise as a result of different speeds between the generator rotor and the turbine shaft. Turbine and generator self-damping can be neglected and the resulting mathematical models are given by [24, 25].

$$\frac{dw_t}{dt} = \frac{1}{2H_t}(T_m - T_s) \tag{5}$$

$$\frac{1}{w_{abs}} \frac{d(\theta_t - \theta_r)}{dt} = w_t - w_r \tag{6}$$

$$T_s = K_s(\theta_t - \theta_r) + D_t \frac{d(\theta_t - \theta_r)}{dt} \tag{7}$$

Where;

H_t = Inertia constant of the turbine, K_s = Stiffness constant; w_t and w_r are turbine and generator rotor speeds in per units; θ_t and θ_r are turbine and generator angular displacements in rad; T_s = shaft torque.

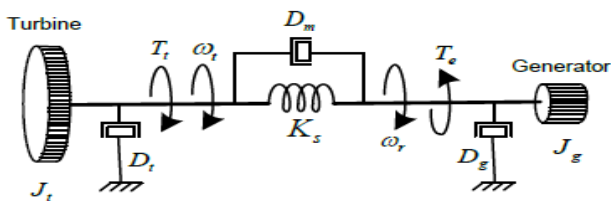


Figure 3. Two-mass drive train model of a wind turbine

III. OPERATION AND ANALYSIS OF ZSI

In Figure 1, the Z-source inverter employs an X-shape LC network between the DC input voltage and the

inverter bridge. The dc source can be either a voltage or a current source, so the dc source can be a battery, rectifying diode, thyristor converter, fuel cell, an inductor, a capacitor, or a combination of those [15, 16].

The theory of active and zero states (vectors) is fundamental in comprehending the working strategy and control of the ZSI. The three-phase ZSI bridge shown in figure 1 has nine allowable switching states unlike the traditional three-phase VSI that has eight. Out of these eight vectors, six are active (i.e. ensuring power delivering to the load) while two are in null states (i.e. the load is shorted through the three upper switches or the three lower switches). However, the three-phase ZSI bridge has one extra zero vector called shoot-through zero vector which is prohibited in the traditional VSI, for the reason that it would lead to a short circuit and hereafter destroy the load. This shoot-through zero vector can be generated in seven distinct ways as follows;

- i. when the load is shorted through both the upper and lower switches of any one phase leg which represents three possible states.
- ii. combination of both lower and upper switches of any two-phase legs (three possible states) and
- iii. all the three phase legs (one possible state).

The effectiveness and efficiency of the ZSI is dependent on the manner in which the switching vectors are incorporated and on the number of times the shoot through vectors are used [26]. Table 1 summarises the possible shoot through states for three phase ZSI.

TABLE 1. POSSIBLE SHOOT THROUGH STATES

| switches | S_{ap} | S_{an} | S_{bp} | S_{bn} | S_{cp} | S_{cn} | ST leg (s) |
|----------|----------|-----------|----------|-----------|----------|-----------|------------|
| ST1 | 1 | 1 | B | \bar{B} | C | \bar{C} | A |
| ST2 | A | \bar{A} | 1 | 1 | C | \bar{C} | B |
| ST3 | A | \bar{A} | B | \bar{B} | 1 | 1 | C |
| ST4 | 1 | 1 | 1 | 1 | C | \bar{C} | AB |
| ST5 | 1 | 1 | B | \bar{B} | 1 | 1 | AC |
| ST6 | A | \bar{A} | 1 | 1 | 1 | 1 | BC |
| ST7 | 1 | 1 | 1 | 1 | 1 | 1 | ABC |

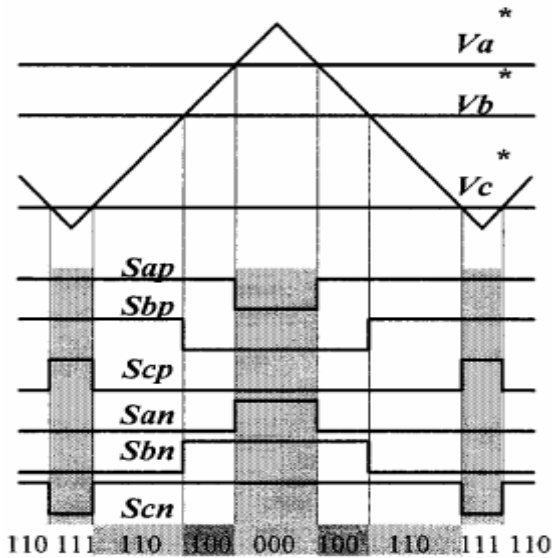


Figure 4. PWM Control V-source inverter

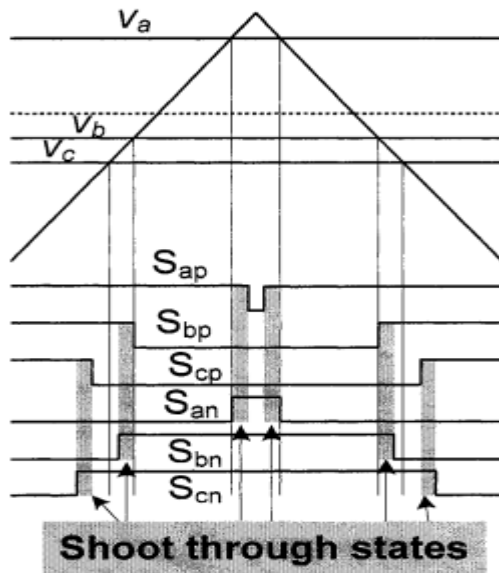


Figure 5. PWM Control of ZSI

All the PWM techniques used in traditional inverters are still valid for the control of ZSI and their theoretical input and output relationship still hold. Fig. 4 illustrates the traditional PWM switching sequence that is derived using triangular carrier approach. Figure 4 is used when DC input is sufficient enough to produce the required AC output voltage and conversely, revised PWM incorporating shoot-

through zero vectors shown in figure 5 is used when the DC input is low, probably as a result of low wind speed to appropriately generate the needed AC output voltage [15, 16]. A comprehensive operational principle can be obtained in [16]. The voltage stress across the switches is defined as the maximum dc-link voltage across the inverter bridge [20] and is expressed as;

$$\hat{v}_i = B \cdot v_o \tag{8}$$

Where B is the Boost factor expressed as;

$$B = \frac{1}{1-2\frac{T_o}{T}} \geq 1 \tag{9}$$

the output peak phase voltage of the inverter is defined as;

$$\hat{v}_{ac} = M \cdot \frac{v_i}{2} = M \cdot B \cdot \frac{v_o}{2} \tag{10}$$

Where M is the modulation index, T_o is the shoot through time per cycle and T is the switching period per cycle.

Equation (10) indicates that the output voltage can be stepped up and down by selecting a suitable buck-boost factor B_B ,

$$B_B = M \cdot B = (0 - \infty) \tag{11}$$

From (10), the voltage gain (G) also called buck-boost factor is expressed as;

$$G = \frac{\hat{v}_{ac}}{v_o/2} = MB \tag{12}$$

IV. MAXIMUM BOOST PWM CONTROL SCHEME

This section discusses the proposed maximum boost PWM control scheme for the ZSI used in the WECS applications. In order to optimally use the zero vectors to lower the voltage stress across the device, maximum boost control approach is used to turn the entire zero vectors of the traditional inverters into shoot through vectors while still maintaining the six active vectors unaffected [7, 27]. Figure 6 illustrates a sketch map for maximum boost control approach.

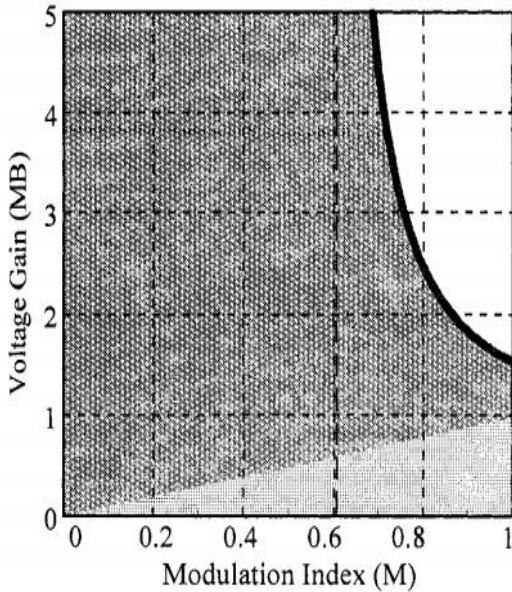


Figure 6. Maximum boost control sketch map

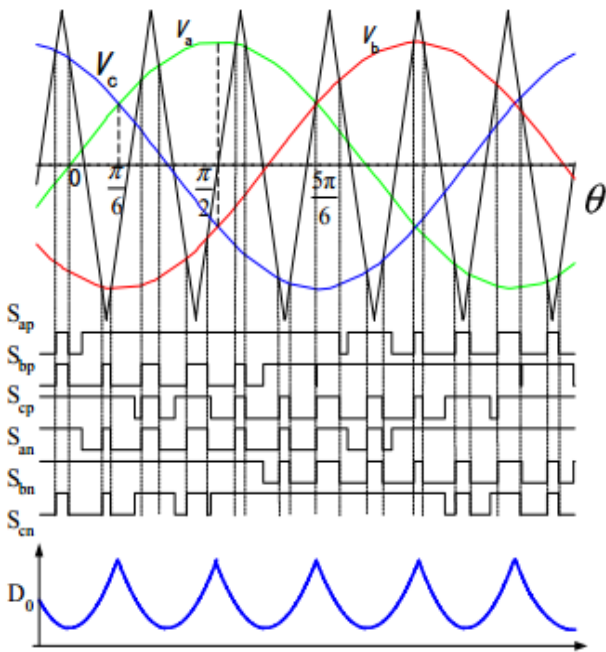


Figure 7. $\frac{\hat{v}_{ac}}{v_o/2}$ versus M

Considerably high voltage stress under a restricted voltage gain in SBC of ZSI is an issue that need to be addressed. MBC scheme is able to reduce voltage stress for any specified voltage gain by lowering the value of B and optimising the value of M while still ensuring that their product is the required value. In the other way, B can be maximised for any modulation index to realise an optimum voltage gain without causing any distortion to the waveform [15].

Thus, the value of shoot through duty ratio needs to be made big (see equation 2).

It is obvious from figure 6, that ZSI is in shoot through condition when the triangular carrier signal is either greater than the peak point of the three-phase sinusoidal reference voltages (V_a, V_b, V_c) or less than the minimum of the references [28]. But, when it is not in any of these conditions, it operates as the conventional traditional inverter [4]. The shoot through duty ratio changes at each cycle and varies at six times of the output frequency. The low frequency current ripples associated with the output frequency are introduced in inductor current and capacitor voltage waveform [29] and this will subsequently lead to increase requirement for the size of the inductors and capacitors.

Figure 8 illustrates the implementation diagram of MBC scheme. The shoot through pulses are incorporated into the switching wave form by logical OR gate. In other to generate the switching pulses, three phase reference voltages are compared with high frequency carrier signal. Comparator compare these two signals and generate pulses. If V_p and V_n are the peak and minimum points of the modulating waveform respectively, and V_{tri} is the amplitude of the triangular carrier signal, then the generated pulse is such that when;

$$\begin{cases} V_p > V_{tri} & \text{ON Pulses} \\ V_n > V_{tri} & \text{OFF Pulses} \end{cases}$$

The pulses produced are then used to turn ON and turn OFF the gate of the power switches in the desired version (24).

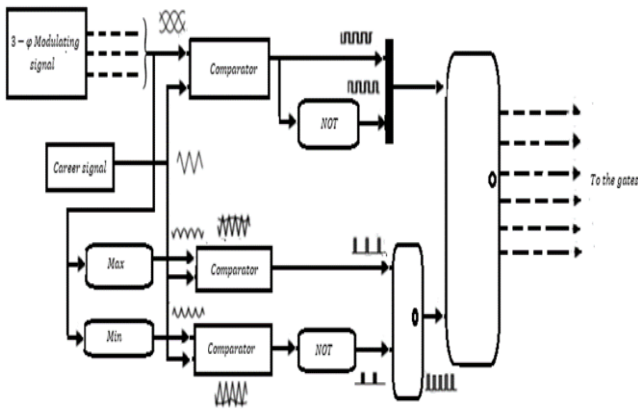


Figure 8. Implementation block diagram of MBC

One parameter that is of great concern while trying to evaluate voltage gain is the average shoot through duty ratio. The shoot through states recurs periodically every $\pi/3$. Suppose that the switching frequency is massively greater than the modulation frequency, the shoot-through duty ratio over one switching cycle in the interval $(\pi/6, \pi/2)$ can be stated as;

$$\frac{T_o(\theta)}{T} = \frac{2 - [M \sin \theta - M \sin(\theta - \frac{2\pi}{3})]}{2} \tag{13}$$

The average duty ratio of shoot-through is evaluated by integrating (13) which yield;

$$\frac{T_o}{T} = \frac{\int_{\frac{\pi}{6}}^{\frac{\pi}{2}} 2d\theta - [\int_{\frac{\pi}{6}}^{\frac{\pi}{2}} M \sin \theta d\theta - \int_{\frac{\pi}{6}}^{\frac{\pi}{2}} M \sin(\theta - \frac{2\pi}{3}) d\theta]}{\int_{\frac{\pi}{6}}^{\frac{\pi}{2}} 2d\theta} = \frac{2\pi - 3\sqrt{3}M}{2\pi} \tag{14}$$

the boost factor is defined as follows;

$$B = \frac{1}{1 - 2\frac{T_o}{T}} = \frac{\pi}{3\sqrt{3}M - \pi} \tag{15}$$

Using this kind of control scheme, the voltage gain can be established through the modulation index M as follows;

$$\frac{\hat{v}_{ac}}{v_o/2} = M.B = \frac{\pi M}{3\sqrt{3}M - \pi} \tag{16}$$

The graph of $\frac{\hat{v}_{ac}}{v_o/2}$ against M is illustrated by the thick curve in figure 7. The shaded portion in the illustration is the probable region of operation of this control scheme. It is clear from figure 7 that there is an inverse relationship between output voltage and

the modulation index M . As M advances to $\frac{\pi}{3\sqrt{3}}$, the output voltage tends toward infinity.

Comparing (12) and (16), the maximum obtainable modulation index for a specific voltage gain is expressed as;

$$M = \frac{\pi B_B}{3\sqrt{3}B_B - \pi} \tag{17}$$

Thus, the voltage stress is,

$$V_s = Bv_o = \frac{\pi v_o}{3\sqrt{3}M - \pi} = \frac{3\sqrt{3}B_B - \pi}{\pi} v_o \tag{18}$$

Fig. 9 and fig. 10 respectively shows the voltage stress in the SBC and MBC. It is obvious from the illustrations that the voltage stress in the proposed control scheme is considerably less than that of SBC technique.

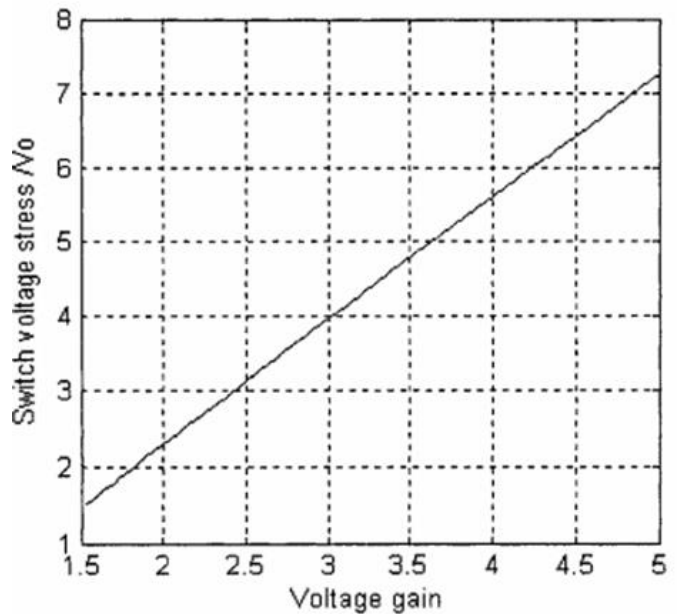


Figure 9. Switch voltage stress VS voltage gain of SBC

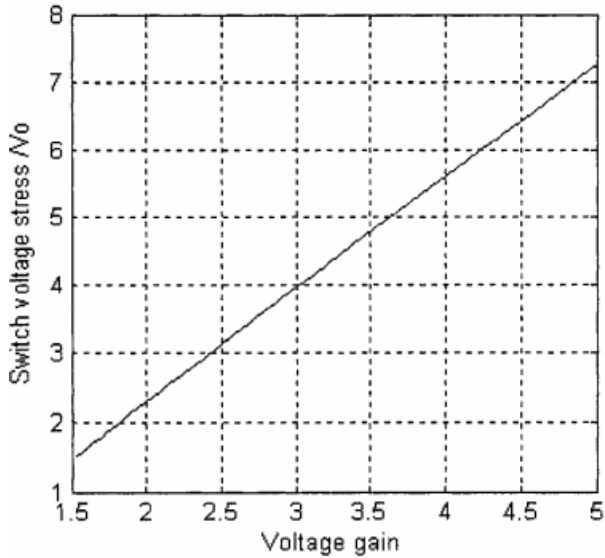


Figure 10. Switch voltage stress VS voltage gain of MBC

V. SIMULATION AND RESULTS

MATLAB 16 was used to simulate the system and the results of the input and output voltages, inductor and output current and the power coefficient have been reported. Fig. 11 represents the simulation results of C_p Vs λ for several blade pitch angle. This curve shows that for every value of β , there is an optimum point at which aerodynamic power is maximum which corresponds to a particular lambda. The plot show that aerodynamic efficiency is maximum at $\beta = 0$, which corresponds to a

$$C_{p(optimum)} = 0.48 \text{ and } \lambda_{opt} = 8.$$

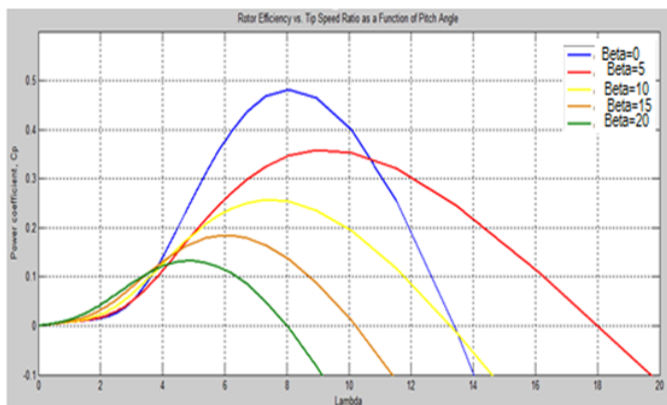


Figure 11. $C_p(\lambda, \beta)$ characteristics for various value of pitch angle

However, the result obtained validate Bertz law which says that the maximum C_p cannot be greater than 0.593 and is only obtainable at beta=0, this is as a result of the various aerodynamic losses depending on rotor construction. Fig. 12 shows the simulation results of PMSG based wind turbine system at a wind speed of 9m/s.

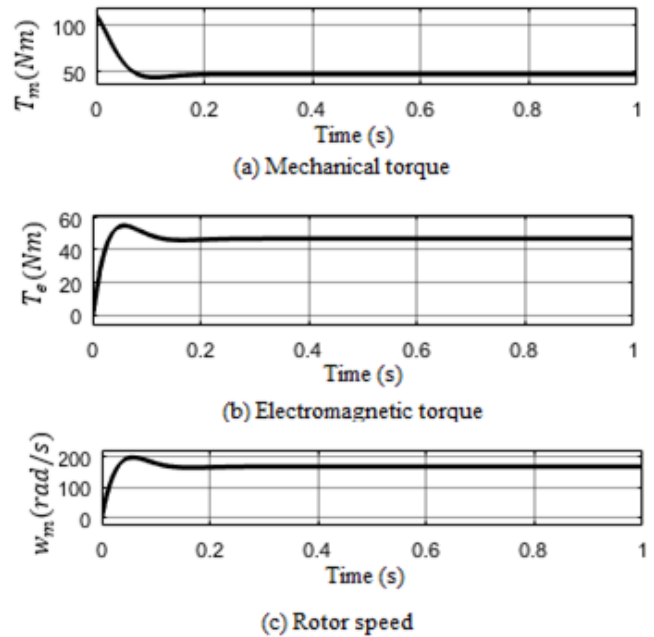


Figure 12. PMSG based wind turbine at $w_s = 9m/s$

Fig. 12(a), Fig. 12(b), Fig. 12(c) respectively represents the mechanical torque, electromagnetic torque and rotor speed of the PMSG.

Simulation was further carried out to authenticate the validity of the maximum boost control technique of three phase ZSI with the following Z-source network parameters: $L_1 = L_2 = 650\mu H$ and $C_1 = C_2 = 1mF$; Switching frequency = $10KHz$ and Modulation index of 0.80 . The wind speed was set at 9 m/s at $\beta = 0$. Figure 13 shows the simulated results prior to the inversion of the DC signal to AC signal.

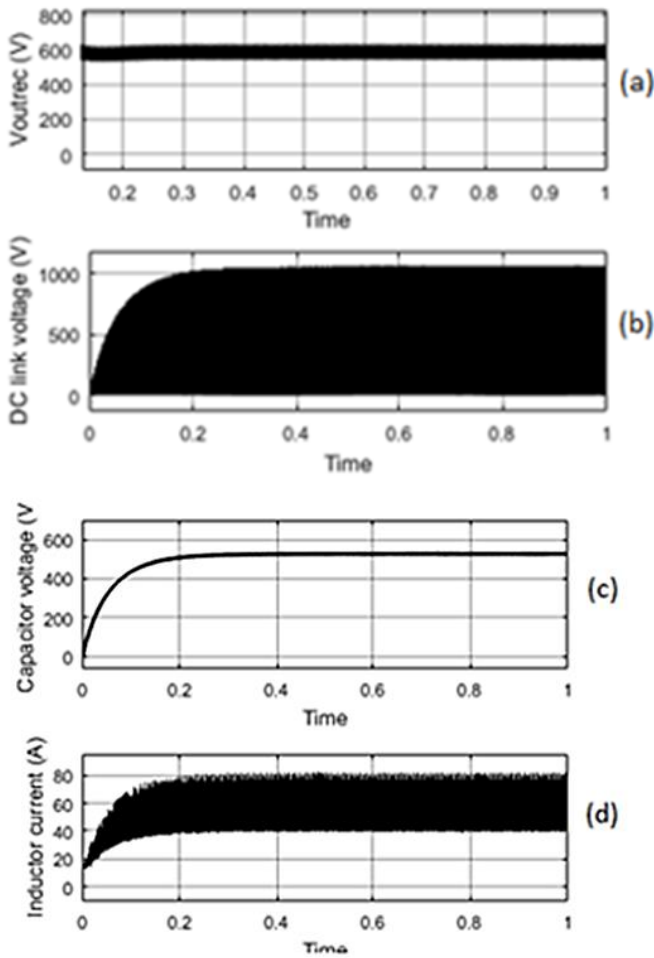


Figure 13. Z-source network simulated parameters (a) Rectifier output voltage (b) DC link voltage (c) Capacitor voltage V_{C2} (V) (d) Inductor current I_{L1} (A)

Fig. 13 (a) is the DC output voltage of the rectifier which also equals the input voltage to the Z-source network while fig. 13 (b) is the DC input to the inverter stage. It is obvious from these two results obtained that boost characteristic has taken place. Fig. 13(c) represent typical exponential rise in the voltage build-up of a capacitor. It is evident from fig. 12 (d) that there is low frequency ($6w$) harmonics in the inductor current which is due to the fact that shoot through in maximum boost control technique is not always constant but varies in each switching cycle.

Fig .14 is the A.C output of the inverter at wind speed of 9m/s and $M=0.8$

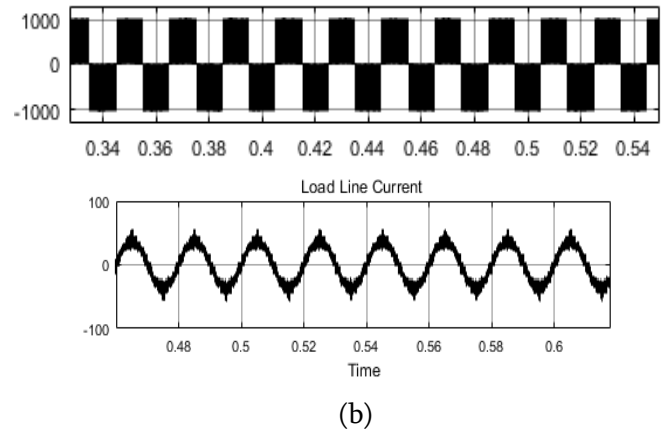


Figure 14. Inverter bridge (a) Output line voltage (V) (b) load current (A)

VI. CONCLUSION

In this paper, the need to insert shoot through in the control scheme has been studied. The relationship between voltage boost and modulation index have also been established. However, it is evident from the results obtained that at a higher wind speed, the output voltage of the PMSG increases and therefore a lesser boost factor with increased modulation index will be required. The results have also shown that boost operation with Z-source inverter is possible without the need for additional boost circuitry, thereby reducing cost and making the system more compact. It is evident from the result obtained that there is low frequency ($6w$) harmonics in the inductor current which is due to the fact that shoot through in maximum boost control technique is not always constant but varies in each switching cycle.

VII. REFERENCES

- [1]. Marisarla, C. and K.R. Kumar, A Hybrid Wind and Solar Energy System with Battery Energy Storage for an Isolated System. International Journal of Engineering and Innovative Technology (IJEIT) Volume, 2013. 3: p. 99-104.
- [2]. Ye, H., J. Su, and S. Du, Simulation and Analysis of PMSG-based Wind Energy Conversion

- System using Different Converter Models. *Engineering*, 2013. 5(01): p. 96.
- [3]. Supatti, U. and F.Z. Peng. Z-source inverter based wind power generation system. in *International Conference on Sustainable Energy Technologies (ICSET) 2008*. 2008. IEEE.
- [4]. Suresh, L., et al., Simulation of Z-Source Inverter Using Maximum Boost Control PWM Technique. *International Journal of Simulation Systems*, 2013. 7(2): p. 49-59.
- [5]. Mosalam, H.A., R.A. Amer, and G. Morsy, Fuzzy logic control for a grid-connected PV array through Z-source-inverter using maximum constant boost control method. *Ain Shams Engineering Journal*, 2018. 9(4): p. 2931-2941.
- [6]. Sabeur, N., S. Mekhilef, and A. Masaoud, A Simplified Time-Domain Modulation Scheme-Based Maximum Boost Control for Three-Phase Quasi-Z Source Inverters. *IEEE Journal of Emerging and Selected Topics in Power Electronics*, 2018. 6(2): p. 760-769.
- [7]. Shen, M., et al. Comparison of traditional inverters and Z-source inverter. in *Power Electronics Specialists Conference, 2005. PESC'05. IEEE 36th. 2005*. IEEE.
- [8]. Nguyen, M.-K., T.-T. Tran, and Y.-C. Lim, A family of pwm control strategies for single-phase quasi-switched-boost inverter. *IEEE Transactions on Power Electronics*, 2019. 34(2): p. 1458-1469.
- [9]. Abbasi, M., A.H. Eslahchi, and M. Mardaneh, Two Symmetric Extended-Boost Embedded Switched-Inductor Quasi-Z-Source Inverter With Reduced Ripple Continuous Input Current. *IEEE Transactions on Industrial Electronics*, 2018. 65(6): p. 5096-5104.
- [10]. Tran, Q.-V., et al., Algorithms for controlling both the DC boost and AC output voltage of Z-source inverter. *IEEE Transactions on Industrial Electronics*, 2007. 54(5): p. 2745-2750.
- [11]. Uthirasamy, R. and U. Ragupathy. Design and realization of maximum boost Z-source inverter for solar power applications. in *Electronics, Computing and Communication Technologies (CONECCT), 2013 IEEE International Conference on*. 2013. IEEE.
- [12]. Shen, M., et al., Constant boost control of the Z-source inverter to minimize current ripple and voltage stress. *IEEE transactions on industry applications*, 2006. 42(3): p. 770-778.
- [13]. Sun, D., et al., Analysis and control of quasi-Z source inverter with battery for grid-connected PV system. *International Journal of Electrical Power & Energy Systems*, 2013. 46: p. 234-240.
- [14]. Shen, M., et al., Comparison of traditional inverters and Z-source inverter for fuel cell vehicles. *IEEE Transactions on Power Electronics*, 2007. 22(4): p. 1453-1463.
- [15]. Miaosen, S. Z-source inverter design analysis and its application in fuel cell vehicles. in *Ph. D. dissertation, Michigan State Univ. 2007*.
- [16]. Peng, F.Z., Z-source inverter. *Industry Applications, IEEE Transactions on*, 2003. 39(2): p. 504-510.
- [17]. Ellabban, O. and J. Van Mierlo, Z-Source Inverter for Automotive Applications, in *New Generation of Electric Vehicles. 2012, InTech*.
- [18]. Do, D.-T. and M.-K. Nguyen, Three-Level Quasi-Switched Boost T-Type Inverter: Analysis, PWM Control, and Verification. *IEEE Transactions on industrial electronics*, 2018. 65(10): p. 8320-8329.
- [19]. Ellabban, O., J. Van Mierlo, and P. Lataire. Comparison between different PWM control methods for different Z-source inverter topologies. in *2009 13th European Conference on Power Electronics and Applications. 2009*. IEEE.
- [20]. Shen, M., et al. Maximum constant boost control of the Z-source inverter. in *Industry Applications Conference, 2004. 39th IAS Annual Meeting. Conference Record of the 2004 IEEE. 2004*. IEEE.
- [21]. Al-Bahadly, I., *Wind Turbines. 2011, InTech*.

- [22]. Samanvorakij, S. and P. Kumkratug. Modeling and Simulation PMSG based on Wind Energy Conversion System in MATLAB/SIMULINK. in Proc. of Second Intl. Conf. on Advances in Electronics and Electrical Engineering. 2013.
- [23]. Eltamaly, A.M., A. Alolah, and H.M. Farh, Maximum Power Extraction from Utility-Interfaced Wind Turbines. 2013.
- [24]. David, P.P., Sustainable Power Production and Transportation. Assignment II, in Chalmers University of Technology, Sweden. 2010.
- [25]. Aliprantis, D., et al. Modeling and control of a variable-speed wind turbine equipped with permanent magnet synchronous generator. in International Conference on Electrical Machines, Helsinki, Finland. 2000.
- [26]. Huang, Y., et al., Z-source inverter for residential photovoltaic systems. IEEE Trans. Power Electron, 2006. 21(6): p. 1776-1782.
- [27]. Shen, M., et al. Maximum constant boost control of the Z-source inverter. in Conference Record of the 2004 IEEE Industry Applications Conference, 2004. 39th IAS Annual Meeting. 2004. IEEE.
- [28]. Ellabban, O. and J. Van Mierlo, Z-Source Inverter for Automotive Applications. 2012.
- [29]. Thangaprakash, S. and A. Krishnan, Implementation and critical investigation on modulation schemes of three phase impedance source inverter. Iranian Journal of Electrical and Electronic Engineering, 2010. 6(2): p. 84-92.

Cite this article as :

Sanusi Alabi Kamilu, AbdulHakeem Mohammed, Bello Ummai, Solomon Ikuforiji, Adebayo Michael, AbdulKadir Muyeideen, "Maximum Boost PWM Control Technique of Three Phase ZSI Based Wind Energy Conversion Systems", International Journal of Scientific Research in Science, Engineering and Technology (IJSRSET), Online ISSN : 2394-4099, Print ISSN : 2395-1990, Volume 6 Issue 5, pp. 191-201, September-October 2019. Available at doi : <https://doi.org/10.32628/IJSRSET196536>
Journal URL : <http://ijsrset.com/IJSRSET196536>